

# INFERRING SUBSURFACE SUPERGRANULAR FLOW DIRECTLY FROM HELIOSEISMIC CORRELATION DATA

M. F. Woodard

*NorthWest Research Associates Inc., CoRA Division, 3380 Mitchell Lane, Boulder, CO 80301-5410, USA*

## ABSTRACT

I will describe the theory and application of direct-modeling analysis, also known as statistical waveform analysis, to the problem of mapping subphotospheric flow. An inversion for supergranular flow, based on a recently-improved forward model for helioseismic correlation data, suggests that the photospheric supergranulation pattern persists to a depth of roughly six megameters, consistent with other recent findings of helioseismology and with numerical simulations of supergranular-scale convection.

Key words: Sun: interior; Sun: mass flows; Sun: seismology.

## 1. INTRODUCTION

Horizontally- and temporally-varying subsurface structures, e.g., flows and magnetic structures, induce correlation between distinct Fourier components of photospheric wave motion. Reference [1] showed how raw correlation measurements can be used directly in an inversion for subsurface supergranular-scale flow. For this inversion, which used a SOHO/MDI high-resolution Doppler data cube covering an approximately 210 Mm by 210 Mm corotating field of view near the center of the solar disk, a time- and depth-independent flow was assumed. The inversion of correlation data is based on a physical model of randomly-driven solar oscillations in a plane-parallel, but otherwise realistic, stellar envelope with weak perturbing flows. The weakness of the perturbation implies a linear dependence of data on subsurface flow velocity. The linear sensitivity calculations have recently been extended to model the effect of depth- and time-dependent flow. I will describe a recent inversion based on the more general sensitivity calculations, which reveals the depth dependence of the flow. I will discuss the vertical resolution and noise properties of the inversion.

## 2. FORWARD MODELING

The inversion uses correlation data in the form  $\hat{\phi}_{\mathbf{k}'\omega'} \hat{\phi}_{\mathbf{k}\omega}^*$ , where  $\hat{\phi}_{\mathbf{k}\omega} = \phi_{\mathbf{k}\omega} / \sqrt{P_{\mathbf{k}\omega}}$  is the horizontal-wave-vector and frequency decomposition of the photospheric vertical velocity (Doppler) measurements divided by root  $P_{\mathbf{k}\omega} = E[|\phi_{\mathbf{k}\omega}|^2]$ , the expected  $\mathbf{k} - \omega$  spectrum (limit spectrum) of the measurements. In the Born approximation, appropriate for weak flows, correlation data depend linearly on the flow velocity.

As an approximation, only poloidal flows with non-divergent mass flux were considered in this study. A convenient way to represent such flows is

$$\rho(z) \mathbf{u}_{\mathbf{q}\sigma} = \sum_m a_{m\mathbf{q}\sigma} [\hat{\mathbf{z}} q^2 \gamma_m(z) + i\mathbf{q} \frac{d\gamma_m(z)}{dz}], \quad (1)$$

where  $\mathbf{u}_{\mathbf{k}\omega}$  is the Fourier component of the flow velocity at height  $z$  above the photosphere,  $\rho(z)$  is the mass density,  $\gamma_m(z)$  are a set of vertical basis functions, and  $a_{m\mathbf{q}\sigma}$  are arbitrary coefficients. For this work, the vertical functions were defined by  $\rho^{-1} d\gamma_m/dz = t_m(z)$ , where  $t_m$  are Chebyshev polynomials of the first kind, and by the condition  $\gamma_m(z_{\max}) = 0$ , where  $z_{\max} = 0.479\text{Mm}$ . The condition at  $z_{\max}$  implies that the vertical mass flux vanishes there. A flow of the form (1) is completely determined by its horizontal divergence,  $D(x, y, z)$ , whose Fourier representation is  $D_{\mathbf{q}\sigma}(z) = i\mathbf{q} \cdot \mathbf{u}_{\mathbf{q}\sigma} = -q^2 \sum_m a_{m\mathbf{q}\sigma} t_m(z)$ . The components  $D_{\mathbf{q}\sigma}(z)$  can therefore be used as an alternative set of flow variables.

The data sensitivity can be written in the general form

$$E[\hat{\phi}_{\mathbf{k}'\omega'} \hat{\phi}_{\mathbf{k}\omega}^*] = \sum_m \hat{K}_{\mathbf{k}'\omega', \mathbf{k}\omega}^{(m)} a_{m(\mathbf{k}'-\mathbf{k})(\omega'-\omega)}, \quad (2)$$

with

$$\hat{K}_{\mathbf{k}'\omega', \mathbf{k}\omega}^{(m)} = \hat{X}_{\mathbf{k}'\omega', \mathbf{k}\omega}^{(m)} + \hat{X}_{\mathbf{k}\omega, \mathbf{k}'\omega'}^{(m)*}. \quad (3)$$

The sensitivity kernel for the present inversions was computed from the approximate expression

$$\hat{X}_{\mathbf{k}\omega, \mathbf{k}'\omega'}^{(m)} = - \sum_{nn'} \frac{w_{n\mathbf{k}\omega} R_{n\mathbf{k}\omega} S_{n\mathbf{k}\omega, n'\mathbf{k}'\omega'}^{(m)} P_{n'\mathbf{k}'\omega'}}{w_{n'\mathbf{k}'\omega'} \sqrt{P_{\mathbf{k}\omega} P_{\mathbf{k}'\omega'}}}, \quad (4)$$

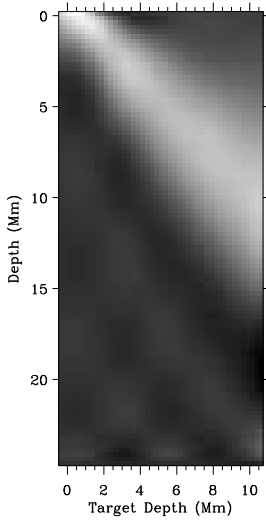


Figure 1. Depth sensitivity,  $R(z, z')$ , as defined by Eq. 6, of the SOLA inversion for  $D_{\mathbf{q}\sigma}(z)$ , as a function of depth  $z'$  for a range of target depths  $z$ . In this example, the wavenumber  $q = |\mathbf{q}|$  of the flow corresponds to angular degree approximately 60. The flow is assumed to be steady (i.e.,  $\sigma = 0$ ).

where  $P_{n\mathbf{k}\omega}$  is the contribution of oscillatory modes of order  $n$  and horizontal wave vector  $\mathbf{k}$  to the power spectrum,  $P_{\mathbf{k}\omega}$ , and  $R_{n\mathbf{k}\omega} = 1/(\omega_{n\mathbf{k}}^2 - \omega^2 - i\omega\gamma_{n\mathbf{k}})$  describes the frequency response of a harmonically-driven, simple, damped oscillator of resonant frequency  $\omega_{n\mathbf{k}}$  and damping rate  $\gamma_{n\mathbf{k}}$  (the mode frequency and damping rate). The quantities  $R_{n\mathbf{k}\omega}$ ,  $P_{n\mathbf{k}\omega}$ , and  $P_{\mathbf{k}\omega} = \sum_n P_{n\mathbf{k}\omega}$  were computed from parameterized fits to oscillation power spectra. The factor  $S_{n\mathbf{k}\omega, n'\mathbf{k}'\omega'}^{(m)}$  in Eq. 4 for the sensitivity kernel is an integral over depth, which quantifies the flow-dependent, dynamical coupling of the oscillation modes of orders  $n$  and  $n'$  and horizontal vectors  $\mathbf{k}$  and  $\mathbf{k}'$ . The plane-parallel envelope used for the computation of the coupling factor was based on solar model S of [2]. The quantity  $w_{n\mathbf{k}\omega} = -i\omega O_{\mathbf{k}} V_{n\mathbf{k}}^{(o)}$ , where  $O_{\mathbf{k}}$  is the instrumental optical transfer function (OTF) and  $V_{n\mathbf{k}}^{(o)}$  is the mode eigenfunction at the height in the solar atmosphere where the Doppler signal is observed by MDI. A derivation of the above sensitivity kernel is given in [3].

The linear model dependence can be expressed in the concise form

$$E[\mathbf{y}] = \hat{\mathbf{K}} \mathbf{u}, \quad (5)$$

where  $\mathbf{y}$ ,  $\hat{\mathbf{K}}$ , and  $\mathbf{u}$  respectively stand for the correlation data, the sensitivity kernel  $\hat{K}_{\mathbf{k}\omega, \mathbf{k}'\omega'}^{(m)}$ , and the model parameters  $a_{m\mathbf{q}\sigma}$ . A similar linear relation describes the sensitivity to the flow variables  $\mathbf{u} = D_{\mathbf{q}\sigma}(z)$ .

The fact that the correlation between the observables  $\phi_{\mathbf{k}\omega}$  and  $\phi_{\mathbf{k}'\omega'}$  depends only on  $a_{m(\mathbf{k}'-\mathbf{k})(\omega'-\omega)}$  (Eq. 2)

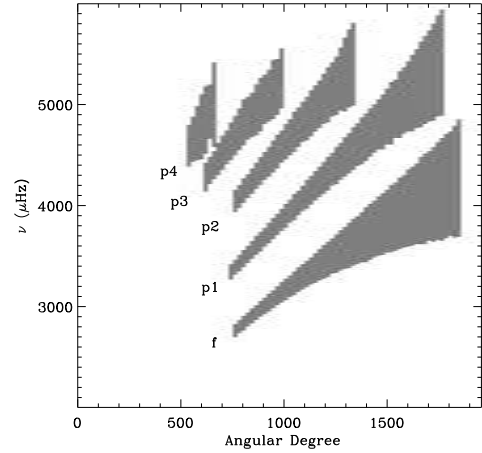


Figure 2. Shaded areas of the  $\ell - \nu$  plane define the regions in  $\mathbf{k} - \omega$  space where the inversions used MDI Doppler signal.

leads to the possibility of inversions by multi-channel decomposition (MCD). That is, inversions for  $a_{m\mathbf{q}\sigma}$  (or  $D_{\mathbf{q}\sigma}(z)$ ) of distinct  $(\mathbf{q}, \sigma)$  can be performed independently of one another.

The realization (stochastic excitation) noise model of [4] was used as the basis for estimating the statistical error of the inversions. As an approximation, the dimensionless correlation data were assumed to have a unit covariance matrix.

### 3. INVERSIONS

Equation 5 was inverted using familiar linear methods, which yield estimates,  $\mathbf{u}' = \mathbf{Q} \mathbf{y}$  of the flow parameters in the form of linear combinations,  $\mathbf{Q} \mathbf{y}$ , of the data. Two methods, regularized least-squares fitting (RLS) and optimally-localized averaging (SOLA), were used in this study. A least-squares estimate depends on the data only through the projections  $\beta = \hat{\mathbf{K}}^\dagger \mathbf{y}$ , a fact which suggests that most of the useful information in correlation data about the flow model resides in  $\beta$ . Furthermore, if the number of vertical basis functions  $\gamma_m$  needed to describe the flow is not terribly large, then  $\beta$  is a much more compact and manageable data set to work with than the correlation estimates. The  $\beta$  are linearly dependent on the model, with sensitivity kernel  $\alpha = \hat{\mathbf{K}}^\dagger \hat{\mathbf{K}}$ , where  $\hat{\mathbf{K}}$  is the sensitivity kernel for correlation data.

The depth dependence of supergranular flow was explored via an SOLA/MCD inversion for the horizontal flow divergence. In the MCD approach, an estimate  $\mathbf{D}' = \mathbf{Q} \beta$ , of  $D \equiv D_{\mathbf{q}\sigma}$  is constructed for each  $\mathbf{q}$  and  $\sigma$ .

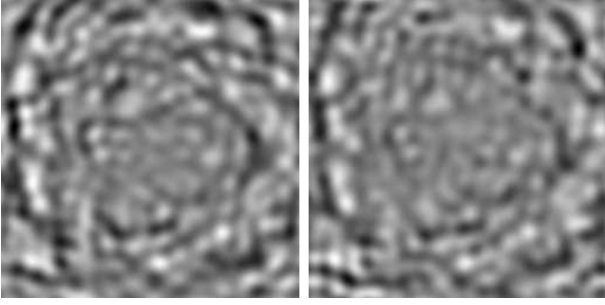


Figure 3. Helioseismically inferred (left) and directly observed (right) supergranular-scale Doppler signal in a 210 Mm by 210 Mm analysis patch near the center of the solar disk.

For this construction one needs theoretical expressions, which can be derived from the forward model, for both the sensitivity of  $D'(z)$  to the model and for the noise in  $D'$ . One finds that

$$E[D'(z)] = \int R(z, z')D(z')dz', \quad (6)$$

with  $\mathbf{Q}$ -dependent depth sensitivity functions (averaging kernels),  $R(z, z')$ . Fig. 1 shows an example of the depth sensitivity of the SOLA inversion. Optimal inverse response kernels,  $\mathbf{Q}$ , were chosen so that  $R(z, z')$ , for fixed sampling height  $z$ , approximated a Gaussian target profile. The correlation data used in the inversions involved Doppler signal  $\phi_{\mathbf{k}\omega}$  such that  $\mathbf{k} = |\mathbf{k}|$  and  $\omega$  lie in regions centered on  $p$ - and  $f$ -mode ridges. The regions used in the inversions, for which the averaging kernels of Fig. 1 are designed, are shown as shaded areas in Fig. 2.

#### 4. ANALYSIS AND RESULTS

Inversions based on the above model were applied to the same 34-hr duration MDI data cube used in the 2002 analysis. As a preliminary step, a least-squares estimate of the supergranular flow was obtained by fitting correlation data to the flow model (Eq. 1), defined by the single depth-independent function  $t_0(z) = 1$ . Least-squares estimates of  $a_{0\mathbf{q}\sigma}$  were thereby obtained for  $\mathbf{q}$  corresponding to the range 50 – 340 of angular degree and  $\sigma$  corresponding to harmonics 0 – 2 of the inverse time span of the data. The least-squares reconstruction of the photospheric Doppler velocity, at the time the moving analysis window framed the center of the solar disk, is shown in Fig. 3. For comparison, a Fourier-filtered version of the Doppler data cube is also shown. (The filter passed the Fourier components  $\phi_{\mathbf{q}\sigma}$  of the data cube for the same  $(\mathbf{q}, \sigma)$  range used in the helioseismic analysis.) The correlation coefficient of the directly-observed and seismically-inferred Doppler maps is 84 % – a significant improvement over the 68 % correlation found in the 2002 analysis, which used only high-degree  $f$ -modes.

The depth dependence of supergranular flow was explored using an SOLA inversion for the horizontal flow

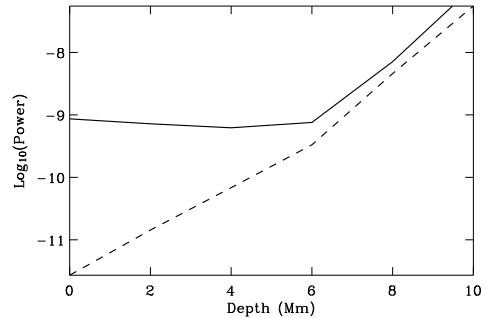


Figure 4. Power, in  $\text{s}^{-2}$ , of the helioseismically-inferred horizontal flow divergence,  $D$ , as a function of subphotospheric depth (solid curve). Theoretical estimate of the noise contribution to the inferred power (dashed curve).

divergence, over the range 0 – 10 Mm of subphotospheric depth, with the same  $(\mathbf{q}, \sigma)$  coverage used in the least-squares inversion. An example of the depth resolution of the inversion is shown in Fig. 1, as discussed above. The solid curve in Fig. 4 shows the total power (mean square variation) in the estimated flow divergence field as a function of depth. Realization noise contributes to the power in the estimated flow and its theoretical contribution is shown by the dashed curve. Comparison of the two curves suggests that we are seeing mainly supergranulation power down to about 6 Mm, but below this depth the measured power is probably dominated by noise. To improve the estimate of supergranulation power, the theoretical noise power was subtracted from the measured power and the corrected power is shown in Fig. 5 along with a replot of the noise contribution. The estimated supergranulation power diminishes gradually with depth over the depth range shown. Recent helioseismic observations suggest that the photospheric supergranulation pattern extends downward 3 to 12 Mm (e.g., [5, 6, 7]). To examine the vertical coherence of the pattern, the cross power of the helioseismically inferred horizontal divergence at the surface and at depth was computed as a function of depth. The resulting  $z$ -dependent cross power (Fig. 5) suggests that the surface pattern persists to at least 6 Mm depth.

#### 5. CONCLUSIONS AND OUTLOOK

The results of this study reinforce the suggestion that supergranular flow extends many megameters into the solar interior. A more detailed helioseismically-based pic-

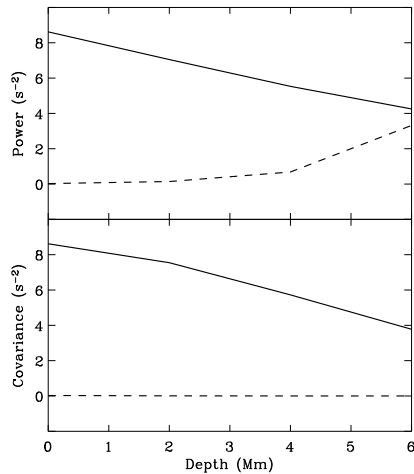


Figure 5. Top panel, solid curve: depth dependence of the estimated power in the horizontal flow divergence, after correction for noise. Top panel, dashed curve: the correction used to obtain the solid curve. Bottom panel, solid curve: estimated cross power (covariance) of the photospheric horizontal flow divergence and the horizontal divergence at depth, as a function of depth. Bottom panel, dashed curve: theoretical noise contribution to the cross power.

ture of subsurface supergranulation will require further improvements in data sensitivity calculations and a better understanding of error. For instance, the treatment of wave excitation and damping used for the current sensitivity calculations is somewhat simplistic and could easily be sharpened. Sources of systematic error include unmodeled features of the solar envelope, such as magnetic or sound-speed perturbations, and assumptions, such as the Born approximation, employed in the sensitivity calculations. A potentially significant source of experimental error, which has yet to be addressed, is aliasing due to limited observational coverage of the solar disk. A proper treatment of aliasing will improve both the sensitivity calculations and the noise model. Analysis of large volumes of helioseismic Doppler data, with increased area coverage, is expected to substantially reduce the random error of the inversions.

## ACKNOWLEDGEMENTS

The author acknowledges Yuhong Fan and Aaron Birch for extensive discussions of helioseismic forward-modeling issues. He thanks Yuhong Fan for participating in the forward-modeling effort and the U.S. National Science Foundation for support under grant ATM 02-23127.

## REFERENCES

- [1] Woodard, M. F., 2002, *ApJ* 565, 634.
- [2] Christensen-Dalsgaard, J. Proffitt, C. R., & Thompson, M. J., 1993, *ApJ* 403, L75.
- [3] Woodard, M. F., 2006, *ApJ* (in press).
- [4] Gizon, L. & Birch, A. C., 2004, *ApJ* 614, 472.
- [5] Duvall, T. L., Jr., 1998, in *SOHO6/GONG98: Structure and Dynamics of the Interior of the Sun and Sun-like Stars*, S. Korzenik and A. Wilson (eds.), ESA SP-418, Noordwijk:ESA, p. 581.
- [6] Zhao, J. & Kosovichev, A. G., 2003, in *Local and Global Helioseismology: The Present and Future*, H. Sawaya-LaCoste (ed.), ESA SP-517, p. 417.
- [7] Braun, D. C., 2003, in *Local and Global Helioseismology: The Present and Future*, H. Sawaya-LaCoste (ed.), ESA SP-517, p. 15.